


# Analysis of the behavior of MVDC system in a distribution grid compared to a UPFC system

Antonio de la Rubia Herrera<sup>1</sup> | Angel L. Zorita-Lamadrid<sup>2</sup> |  
Oscar Duque-Perez<sup>2</sup>  | Daniel Morinigo-Sotelo<sup>2</sup>

<sup>1</sup>Shift Boss Service Operation, Thermal Power Plant "La Pereda", Grupo Hunosa, Oviedo, Spain

<sup>2</sup>Department of Electric Engineering, Research Group ADIRE, Institute ITAP, Universidad de Valladolid, Valladolid, Spain

## Correspondence

Oscar Duque-Perez, Paseo del Cauce 59, Valladolid 47011, Spain.

Email: oscar.duque@eii.uva.es

**Handling Editor:** Dr. Fang, Sidun

## Summary

The increase in electricity demand, the incorporation of renewable energies, or the trend toward deregulation in the power market, implies significant changes in the power networks. Load flows are considerably altered, giving rise to technical problems in the system, such as stability limitations or voltage level control. In this context, the use of devices based on power electronics to interconnect distribution grids is presented as an excellent option to help solve these problems and control load flows and bus voltages. The topology MVDC (Medium Voltage Direct Current) is starting to be considered an option for enhancing transfer capacity and providing increased power quality at distribution grids. However, this technology is still immature and relatively unknown, for this reason, the main motivation of the article is to help spread the benefits of integrating this technology in distribution grid and to determine the capability of the MVDC to control active and reactive power in distribution grid as well as its behavior in the event of a short-circuit. The main novelty is to analyze the behavior of the MVDC through a case study, based on a real situation, but comparing it with one of the most complete and flexible FACTS devices, Unified Power Flow Controller (UPFC), noting that MVDC technology is a better option for operation in medium voltage networks, since allows the control of the active and reactive powers independently and in the case of a short-circuit acts on the currents circulating through the electrical line mitigating the effect caused by the fault.

**List of Symbols and Abbreviations:** C, capacitor DC link; C<sub>2</sub>, coupling capacitor VSC2; FACTS, flexible AC transmission systems; F<sub>res</sub>, switching frequency VSC2; F<sub>res</sub>, switching frequency VSC1; i<sub>1</sub>, input current; i<sub>1d</sub>, input current, d-axis; i<sub>1d</sub><sup>\*</sup>, reference input current, d-axis; i<sub>1q</sub>, input current, q-axis; i<sub>2</sub>, output current; i<sub>2d</sub>, output current, d-axis; i<sub>2d</sub><sup>\*</sup>, reference output current, d-axis; i<sub>2q</sub>, output current, q-axis; i<sub>2q</sub><sup>\*</sup>, reference output current, q-axis; IGBT, insulated gate bipolar transistor; MVDC, medium voltage direct current; P<sub>2</sub>, output active power; P<sub>2</sub><sup>\*</sup>, reference output active power; P<sub>ns</sub>, nominal active power VSC2; P<sub>nsh</sub>, nominal active power VSC1; P<sub>s</sub>, controlled active power; PWM, pulse width modulation; Q<sub>1</sub>, input reactive power; Q<sub>2</sub>, output reactive power; Q<sub>2</sub><sup>\*</sup>, reference output reactive power; Q<sub>s</sub>, controlled reactive power; R<sub>L1</sub>, resistance AC line 1; R<sub>L2</sub>, resistance AC line 2; R<sub>s</sub>, coupling resistance VSC2; R<sub>sh</sub>, coupling resistance VSC1; r<sub>ts</sub>, transformation relation VSC2; r<sub>tsh</sub>, transformation relation VSC1; UPFC, unified power flow converter; v<sub>1</sub>, input voltage; v<sub>2</sub>, output voltage; v<sub>cs</sub>, injected series voltage; v<sub>cd</sub>, series voltage, d-axis; v<sub>cd</sub><sup>\*</sup>, reference series voltage, d-axis; v<sub>cq</sub>, series voltage, q-axis; v<sub>cq</sub><sup>\*</sup>, reference series voltage, q-axis; V<sub>cs</sub>, nominal voltage VSC2; V<sub>csh</sub>, nominal voltage VSC1; v<sub>dc</sub>, direct voltage; VSC, voltage sourced converter; VSC1, voltage sourced converter 1; VSC2, voltage sourced converter 2; X<sub>L1</sub>, reactance AC line 1; X<sub>L2</sub>, reactance AC line 2; X<sub>s</sub>, coupling reactance VSC2; X<sub>sh</sub>, coupling reactance VSC1; θ<sub>1</sub>, phase angle bus 1; θ<sub>2</sub>, phase angle bus 2.

This is an open access article under the terms of the Creative Commons Attribution-NonCommercial-NoDerivs License, which permits use and distribution in any medium, provided the original work is properly cited, the use is non-commercial and no modifications or adaptations are made.

© 2021 The Authors. *International Transactions on Electrical Energy Systems* published by John Wiley & Sons Ltd.

**KEYWORDS**

control strategies, medium voltage direct current (MVDC), optimize power grid, three-phase short-circuit, unified power flow converter (UPFC), voltage sourced converter (VSC)

## 1 | INTRODUCTION

Electric power systems are continuously developing. Nowadays, there is a need for evolution due to the growth of the electric demand in industrialized, and especially, developing countries added to the environmental issues that have led to the continuous integration of renewables energies. However, this growth leads to technical problems, mostly related to stability limits and voltage issues. Due to the inherent variability of renewable energy sources, their integration and deep penetration can significantly affect the electric system.<sup>1,2</sup> The traditional structure of the electric grid is based on power plants located far from the load points, with unidirectional power flow from generation to consumers. However, the context of liberalization of energy markets and the recent evolution toward smart grids raise doubts about the adequate use of electric power systems nowadays. This is especially relevant concerning distribution grids where there is a transition from passive distribution networks to active ones. Distribution grids are now facing requirements to perform as transportation networks providing services such as load flow, contingency analysis, and stability. Besides, future grids will have to meet an increasing demand, the trend toward deregulation, and the increase of distributed generation with its consequences: increase of short circuit power, inverse load flow, and degradation of power quality, including flicker.<sup>3</sup>

To solve these problems, the distribution companies have implemented different measures to optimize the transmission capacity and improve the operability of their networks. Among these measures, the use of FACTS has been offering the best performance for this purpose, being one of the most complete of these devices, the Unified Power Flow Controller (UPFC).<sup>4</sup> These are systems based on power electronics that, with a significant speed of response, allow to regulate the voltage of the node of the network to which they are connected. Besides, these systems allow to compensate the reactive energy, obtaining a greater capacity of control on the power flow, increasing the transference capacity of the network, and damping the power oscillations.<sup>5</sup>

However, the extension of this problem and the advances in power electronics are driving the application of other measures such as the use of Medium Voltage Direct Current (MVDC) links, based on the use of voltage source converters (VSC).

This technology is undergoing significant development for integrated power systems in electric ships (All Electric Ships),<sup>6</sup> in the connection of offshore wind farms,<sup>7</sup> in microgrids, or even proposals for new railway electrification systems can be found based on MVDC.<sup>8,9</sup> But in this paper, its application will be analyzed in the improvement of the operation of electrical grids, since these are MVDC transmission links that allow efficient transmission routes between medium voltage alternating current electricity networks (up to 150 kV), improving the control capacity and flexibility of the entire system. Besides, MVDC can provide controlled power between medium voltage distribution groups, without affecting short-circuit levels, voltage differences, loop flows, or limitations due to phase-angle differences.<sup>10,11</sup> It should also be considered that the implementation of this technology does not necessarily require the construction of new lines since these links can be integrated into existing networks by replacing existing lines, which eliminates the problem of having to make new routes.<sup>12,13</sup>

There are already initiatives in this direction, such as Scottish Power Energy Network's Angle-DC Project, which aims to strengthen the transfer of renewable energy between Anglesey and North Wales mainland (UK) through Europe's first MVDC link.<sup>14,15</sup> Or various studies analyzing the advantages of implementing VDC links in distribution networks, including<sup>16</sup> simulating the behavior of VDC links in order to improve the capacity of the network concerning the incorporation of low-carbon generation technologies and the transition to electric vehicles in a case applied to suburban distribution in Scotland<sup>17</sup>; which shows the advantages of implementing MVDC links as an alternative to AC lines in the Korean electricity system<sup>18</sup>; where the first dual terminal VSC-MVDC distribution network built in China is analyzed<sup>19,20</sup>; where the advantages of the application of these links are shown.

However, despite these examples, it is a developing technology and not well-known. For this reason, and in order to help understand how this technology works, this article proposes a comparative analysis with the UPFC, one of the most complete and flexible FACTS devices, also based on VSC, and which also has independent active and reactive power control capacity.<sup>21</sup> We believe that this novel comparative analysis will help to understand the advantages of the

introduction of MVDC technology in a distribution grid. There is no similar study in the current literature that compares these technologies from the point of view of their behavior, although it does with regard to the relative size of the devices.<sup>22</sup> In this way, this work is intended to cover a research gap that facilitates current and future researchers to know the behavior of this technology by analyzing different control strategies, evaluating the response to changes in reference values; as well as its behavior against a three-phase short-circuit. Economic factors, such as equipment devices, maintenance, or operation cost, have not been considered since the aim is to determine, which topology provides the best independent control of active and reactive power, and which one behaves better in the event of a three-phase short-circuit. Therefore, it will be possible to demonstrate how this technology can help solve the saturation problem that currently exists in distribution grids, especially in developed countries, as indicated above, due to the increase in demand, the increase in distributed renewable generation, and the evolution of the electricity market that seeks to facilitate the incorporation of so-called prosumers (consumers and producers of electricity), and that complicates the operation of these networks.

The structure of the papers is as follows: Section 2 introduces MVDC and UPFC technologies, Section 3 shows the grid under study, Sections 4 and 5 present a comparative analysis of the performance of both topologies, and Section 6 sets out the conclusions.

## 2 | BASIC STRUCTURE OF UPFC AND MVDC SYSTEMS

### 2.1 | UPFC systems

The UPFC is the most versatile of the FACTS devices, providing full dynamic control of transmission parameters of a power system: voltage, line impedance, and phase angle.

UPFC is composed of two VSCs connected to the power system through a coupling transformer. VSC1 is connected in shunt to the transmission system via a shunt transformer, while VSC2 is connected in series through a series transformer.<sup>23,24</sup> Both converters are interconnected in DC, through a set of capacitors. Figure 1 shows a schematic of this topology together with the control blocks required for its operation.

VSC2 injects a voltage of controllable magnitude and phase angle through a transformer in series with the line to control active and reactive power flows on the transmission line. This AC voltage is produced by the switching of DC-fed IGBTs from the link capacitor. The active power exchanged with the line is supplied by the system through the shunt converter and the DC link. The active power can flow freely in both directions between the AC terminals of the two converters.

VSC1 supplies or absorbs the active power demanded by VSC2 through the DC link. VSC1 can also generate or absorb reactive power, thus providing shunt compensation independently of the series converter, allowing local voltage control. For the correct operation of the system, VSC1 must keep the DC link voltage constant, and VSC2 must apply the necessary voltage according to the desired control strategy.

UPFC systems have been researched broadly, and their characteristics have been broadly reported in the literature. Reference 25 shows a recent review about Enhancement of Power Transfer Capability of Interconnected power system using UPFC, and References 24,26-28 are examples where this device can be consulted in more detail. In recent years,

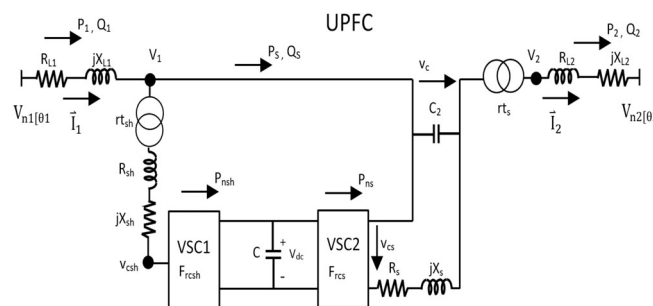


FIGURE 1 UPFC connection diagram

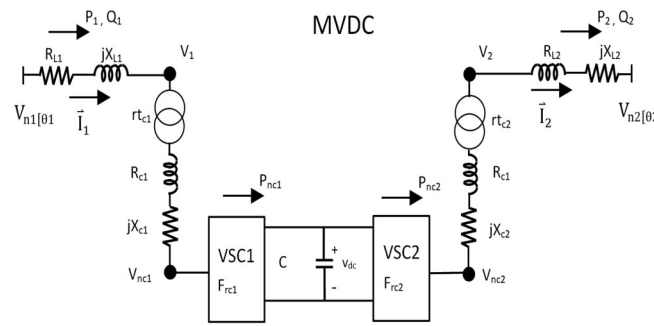


FIGURE 2 MVDC connection diagram

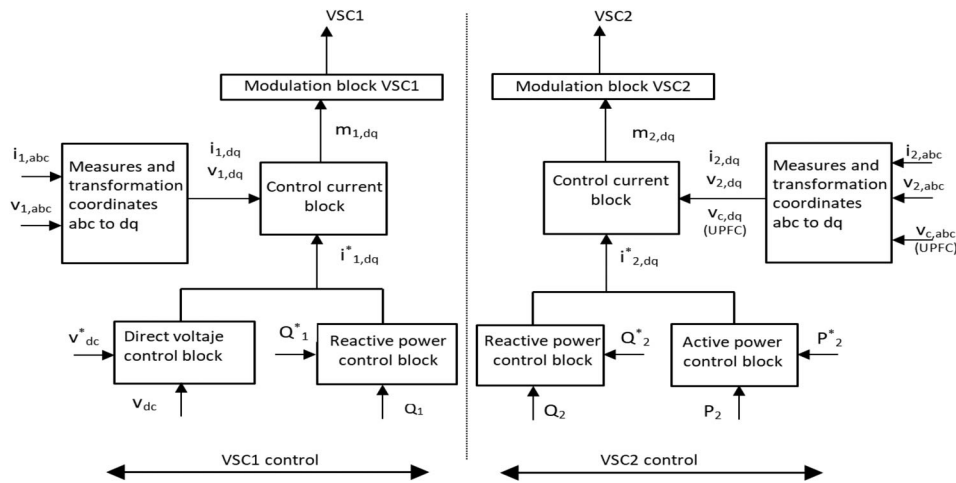


FIGURE 3 Control modules

UPFCs have been widely adopted in China where several UPFC projects have been put into operation in the last 5 years.<sup>29-31</sup>

## 2.2 | MVDC systems

MVDC is starting to be considered an option for enhancing transfer capacity and providing increased power quality at distribution grids.<sup>32,33</sup> MVDC consists of fully-controlled converters. Using MVDC in a configuration of two VSCs connected back to back sharing the same link allows controlling both VSCs independently in a certain power range. MVDC can impose the active power flow between the two AC sides and, simultaneously, can control independently the two AC terminal voltages. Moreover, if needed, an outer reactive power control-loop can be implemented to define proper terminal voltage references.<sup>34, 35</sup> Figure 2 shows a diagram of MVDC topology together with the control blocks required for its operation.

MVDC operation is explained by considering VSC1 and VSC2 as two decoupled converters in which amplitude, phase, and frequency can be controlled independently. VSC1 and VSC2 can function as a rectifier or inverter depending on the direction of the power flow. The active power flow can change at any time and go in any direction. The reactive power can be controlled between VSC1 and VSC2 and their connection grids can be capacitive or inductive. By using the controllable power transfer capability, and individual voltage control capabilities of each converter, it is possible to dynamically force active power flows to balance feeders (and phase loadings). Therefore, the existing network capacity can be better utilized, besides controlling the reactive power in the points of common coupling.

As it has been mentioned in the case of the UPFC, there is also an extensive literature for the description of the MVDC that can be consulted to know its operation in more detail,<sup>36,37</sup> and some more applications in addition to those described in the introduction can be found in Reference 38.

## 2.3 | Control strategies

The mission of the control scheme is to make the MVDC link do what it is told to do. This scheme will count as inputs the states of  $i_1$ ,  $i_2$ , and  $v_{dc}$ , besides measuring also the voltages  $v_1$  and  $v_2$  since it is necessary to know their value at all times, besides  $v_c$  in the case of the UPFC, generating as outputs with two pulse width modulation signals, one for each converter.<sup>39</sup>

The control strategy of UPFC and MVDC is based on three degrees of freedom. The first one is the monitoring and control of the reactive power at the point of connection by VSC1 (Q1). The other two degrees of freedom are used to monitor and control the active and reactive power flow of VSC2 at its point of connection (P2 and Q2) since the active power will be the same between both converters. The restriction preventing four degrees of freedom applies in this case to the VSC1 converter, which will keep the DC link voltage at a constant value, as can be seen in Figure 3.

In the vector control strategy, the Park-Clarke transform is applied. Three-phase currents are transformed into  $d$  and  $q$  axes, which are then synchronized with the three-phase voltage system through the synchronization system block (Figures 1 and 2). The variables  $i_{1d}$ ,  $i_{1q}$ ,  $i_{2d}$ , and  $i_{2q}$ ,  $v_{cd}$ , and  $v_{cq}$ , (Figures 1 and 2) are control parameters of VSC1 and VSC2, generated internally in the control of each converter. Voltages on the  $d$  and  $q$  axes, generated by vector control, are transformed into three-phase quantities and converted to line voltages by the converter.

As will be observed in the following sections, VSC1 internally monitors  $v_{dc}$  and its reactive power can only be controlled by modifying  $i_{1d}$ . Meanwhile, VSC2 modifies its active and reactive power by varying  $i_{2q}$  and  $i_{2d}$  respectively, or by varying  $P_2$  and  $Q_2$ . Only UPFC could modify the active and reactive power varying  $v_{cq}$  and  $v_{cd}$ .

## 3 | CASE STUDY

The paper aims to help to understand how this technology works and to verify the advantages of introducing an MVDC device in a distribution grid for the control of the active and reactive power flow, thus improving the capacity of an existing grid. The behavior of the MVDC link will be compared with other more mature technology and more widely used device such as the UPFC, which is also used to improve the capabilities and performance of distribution networks.

The case study is based on a real situation in a distribution grid in Northern Spain that is saturated, expecting that, in the event of possible future load increases, there could be limitations and overloads in some of the circuits or transformers and even could reach inadequate voltage levels.

To improve network operability, it is proposed to connect two nodes with an MVDC link (Figure 4). The link is created between two nodes that have been selected to maximize the loadability of the system under voltage stability conditions. To select the nodes, a genetic algorithm has been implemented, such as is proposed in References 40,41. In the

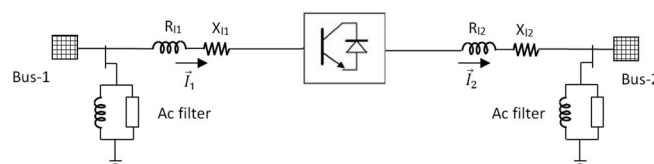


FIGURE 4 Network model

TABLE 1 Data of the case study network for the simulation

Variables	Values	Meaning
$V_{n1}$ - $V_{n2}$	20 kV	Nominal voltages buses 1, 2
$\theta_1$	$0^\circ$	Phase angle bus 1
$\theta_2$	$-3^\circ$	Phase angle bus 2
$I_1$ - $I_2$	400 A	Nominal current AC lines 1 and 2
$R_{L1}$ and $R_{L2}$	1.31 $\Omega$	Resistance AC lines 1 and 2
$X_{L1}$ and $X_{L2}$	0.565 $\Omega$	Reactance AC lines 1 and 2

application of the algorithm, each individual of the working population is composed of three genes representing the system loadability increment, the MVDC connection node, and the active-to-reactive power ratio that the link can support. The chargeability can vary between 0 and 1, and the P/Q ratio between 0 and 2.5, the initial value being chosen randomly for each of the individuals in the population.

Table 1 shows the provided by distribution company corresponding to regular operation in steady-state of the selected link. For the simulation of the behavior of the links, voltages and currents will be in per-unit values. The short-circuit power at bus 1 is 450 MVA, considered the base power for per-unit values of link 1, and at bus 2, 300 MVA is the base power for values per-unit values of link 2.

This work does not try to show the improvement in the behavior of the distribution network itself by incorporating these links, which requires further work, but to see if the MVDC link is a more effective solution than other devices. MVDC and UPFC topologies are analyzed applying different control strategies to check, which of the devices allows better control of the active and reactive power. This analysis is complemented by the simulation of a three-phase short-circuit near one of the converters (one of the most critical contingencies) to check, which of the two topologies best behaves against this fault.

Since real experiments cannot be conducted, it is necessary to use simulation tools to compare and analyze different options with both technologies.<sup>12</sup> In this paper, the tests have been performed with the power system analysis software DIgSILENT PowerFactory.

## 4 | UPFC BEHAVIOR ANALYSIS

### 4.1 | UPFC data

Table 2 indicates the nominal values of the converters, inductances, resistances, and coupling capacitors, which are shown in Figure 1. These data were fixed after consulting with technologists from two companies who were provided with information on the connection points (short circuit power, chargeability, and voltage drops). It should be noted that the nominal voltage of VSC1 is linked to the voltage of the network ( $\vec{V}_1$ ) through the transformer ratio ( $rt_{sh}$ ). The current circulating through the secondary of the parallel transformer is greater than the primary so that the apparent power on both sides of the transformer is the same. In the case of VSC2, its nominal voltage is a fraction of the voltage of the network, and the current on both sides of the series transformer is the same. As a result, the nominal power of the series converter is low, and the power of the parallel converter is dimensioned at the designer's discretion according

TABLE 2 UPFC and MVDC data

Meaning	UPFC variables	UPFC values	MVDC variables	MVDC values
Nominal active power VSC1	$P_{nsh}$	10 MW	$P_{nC1}$	10 MW
Nominal active power VSC2	$P_{ns}$	1 MW	$P_{nC2}$	10 MW
Nominal voltage VSC1	$V_{csh}$	1200 V	$V_{nC1}$	2 kV
Nominal voltage VSC2	$V_{cs}$	1200 V	$V_{nC2}$	2 kV
Transformation relation VSC1	$rt_{sh}$	20 000/1200	$rt_{C1}$	20/2 kV
Transformation relation VSC2	$rt_s$	1/1	$rt_{C2}$	20/2 kV
Coupling reactance VSC1	$X_{sh}$	0.08 pu	$X_{C1}$	0.08 pu
Coupling resistance VSC1	$R_{sh}$	0.01 pu	$R_{C1}$	0.01 pu
Coupling reactance VSC2	$X_s$	0.08 pu	$X_{C2}$	0.1 pu
Coupling resistance VSC2	$R_s$	0.01 pu	$R_{C2}$	0.01 pu
Switching frequency VSC1	$F_{rcsh}$	5000 Hz	$F_{sC1}$	5000 Hz
Switching frequency VSC2	$F_{rcs}$	5000 Hz	$F_{sC2}$	5000 Hz
Voltage DC link	$V_{dc}$	2.5 kV	$V_{dc}$	2 kV
Capacitor DC link	$C$	1000 $\mu$ F		
Coupling capacitor VSC2	$C_2$	100 $\mu$ F		



to the desired degree of reactive power compensation. In this case, the power of VSC1 has been chosen 10 times larger than that of VSC2 so any change in the reference powers of VSC2 will slightly affect the VSC1. Therefore, the result of the VSC1 simulation is only shown once, the result is identical for the rest of the simulations. The difference is in the control strategies used for VSC2.

## 4.2 | Control strategy of VSC1

In this section, the VSC1 control strategy is considered. VSC1 controls the DC link voltage and the reactive power injected at its point of connection ( $Q_1$ ). This means that it only has one degree of freedom ( $Q_1$ ) governed by the reference current  $i_{1d}^*$ . The following procedure must be performed to operate UPFC:

- The DC link is preloaded using an uncontrolled rectifier until a voltage close to the nominal voltage is reached.
- When the voltage is stabilized, the control of the DC link is initiated using the rectifier controlled in the instant 0.02 second at a voltage close to the nominal (Figure 5, top). The reference current  $i_{1d}^*$  must be zero until the DC link voltage is stabilized (0.1 second in this simulation (Figure 5, bottom)).

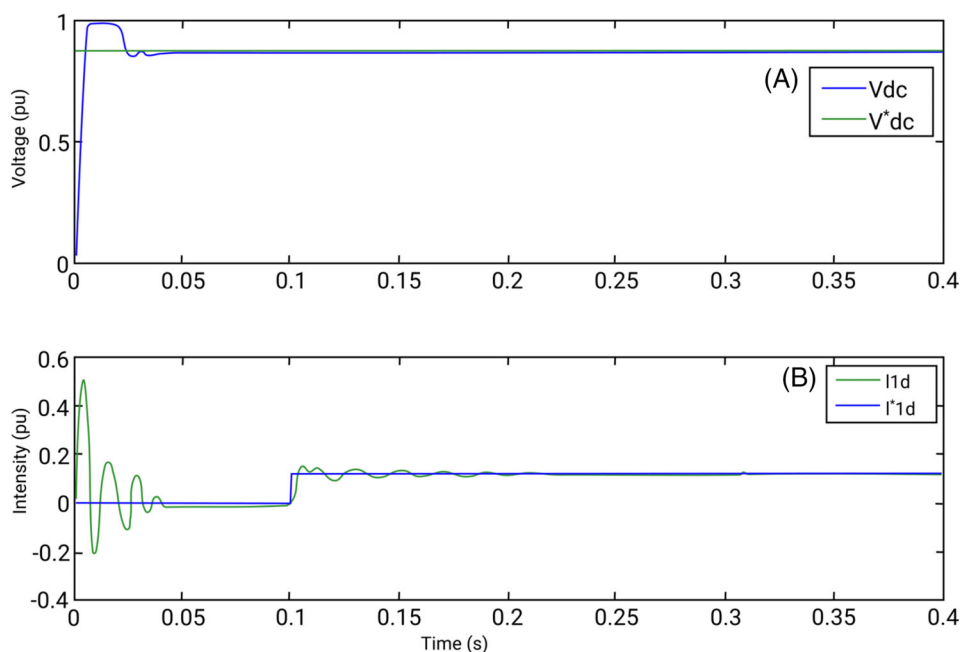


FIGURE 5 Tracking of reference voltage  $v_{dc}^*$  (top) and reference current  $i_{1d}^*$  (bottom)

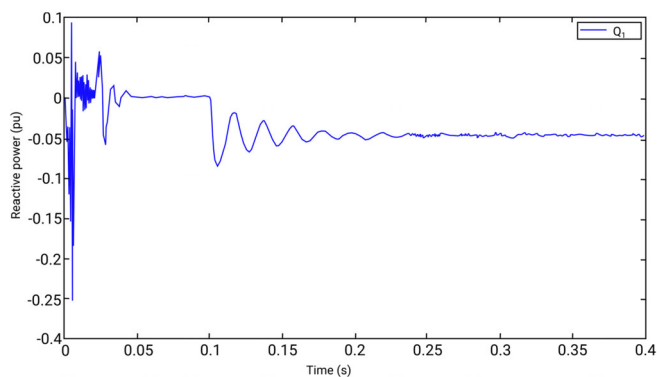


FIGURE 6 Reactive power flow in AC line 1,  $Q_1$

- At 0.1 second, the reference current  $i_{1d}^*$  is changed, thus changing the reactive power injected by this converter (Figure 6). It is observed how the current  $i_{1d}$  allows controlling the reactive power, although this is not achieved until 0.2 second when the IGBTs turn on, when  $i_{1d}$  becomes a stable parameter of control and can follow the reference current  $i_{1d}^*$  (Figure 5, bottom).

### 4.3 | Control strategy of VSC2

In this section: three different control strategies of the series converter are studied: current control, voltage control, and power control.

#### 4.3.1 | Control changing the reference currents

This section shows the simulations corresponding to the control of VSC<sub>2</sub> acting on the reference currents  $i_{2d}^*$  and  $i_{2q}^*$ , whose control is related to the control of  $P_2$  and  $Q_2$ , respectively.

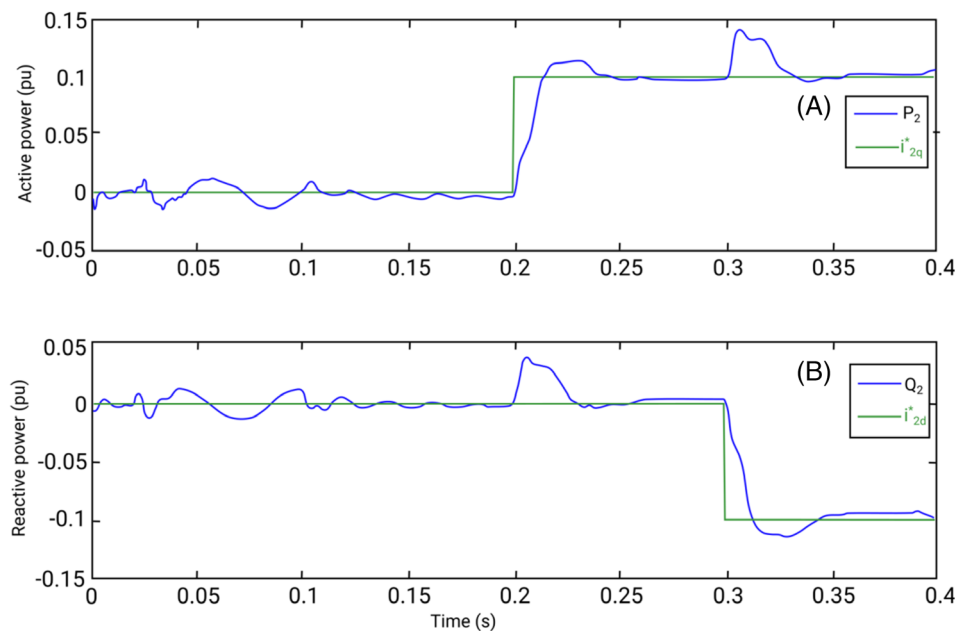


FIGURE 7 Tracking of reference current  $i_{2q}^*$  and active power  $P_2$  (top) and reference current  $i_{2d}^*$  and reactive power  $Q_2$  (bottom)

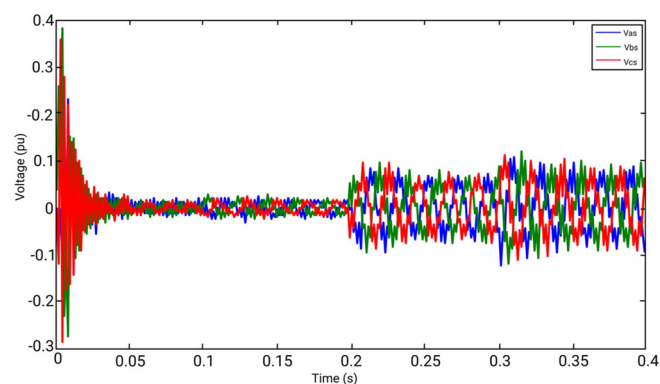


FIGURE 8 Series voltage injected into the system



Following the procedure described in Section 4.2, once the DC link is stabilized at 0.1 second,  $Q_1$  is controlled and stabilized. Then, VSC1 can start to control  $P_2$  and  $Q_2$  indirectly via  $i_{2q}^*$  and  $i_{2d}^*$ . Figure 7 shows the variation of the reference currents and the active and reactive powers  $P_2$  and  $Q_2$ , related to them. Note that  $i_{2q}^*$  and  $i_{2d}^*$  are null until they are changed at 0.2 and 0.3 second, respectively, because until then the only degree of freedom is the control of  $Q_1$  by  $i_{1d}$ . Figure 7 also shows the difficulty of tracking  $i_{2q}^*$  and  $i_{2d}^*$  with this control strategy. There is also a significant coupling between active and reactive powers since a change of the reactive power is reflected in the active one and vice versa.

These results show that the control strategy based on the VSC2 reference currents is not successful because the value of the capacitor C2 (Figure 1) must be decreased to diminish the current flowing toward it. This decrease produces a significant increase in the harmonic content of the injected series voltage (Figure 8), affecting the controller.

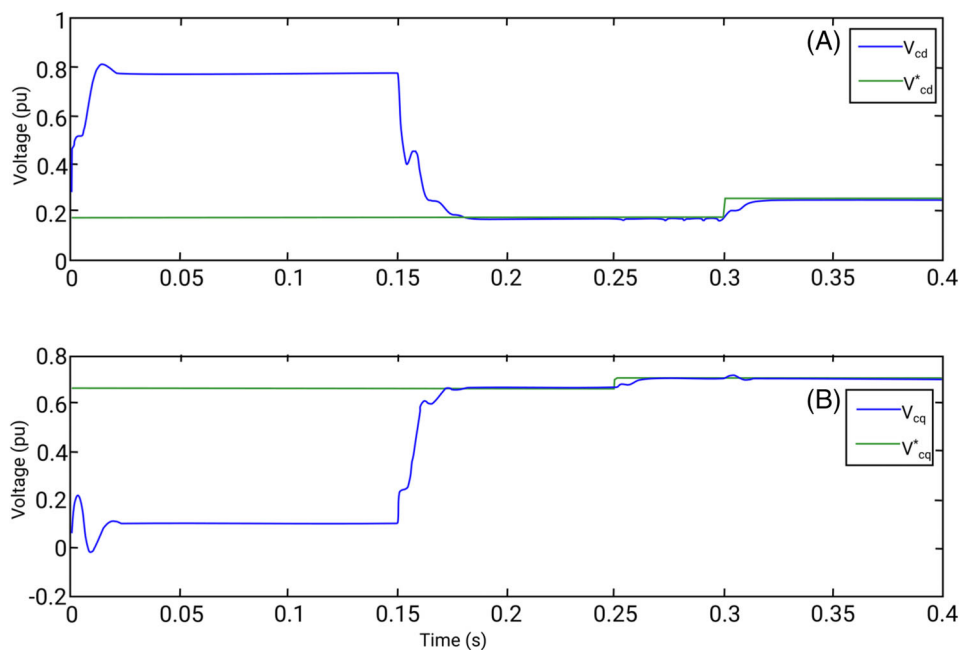


FIGURE 9 Tracking of references voltages  $v_{cd}^*$  (top) and references voltages  $v_{cq}^*$  (bottom)

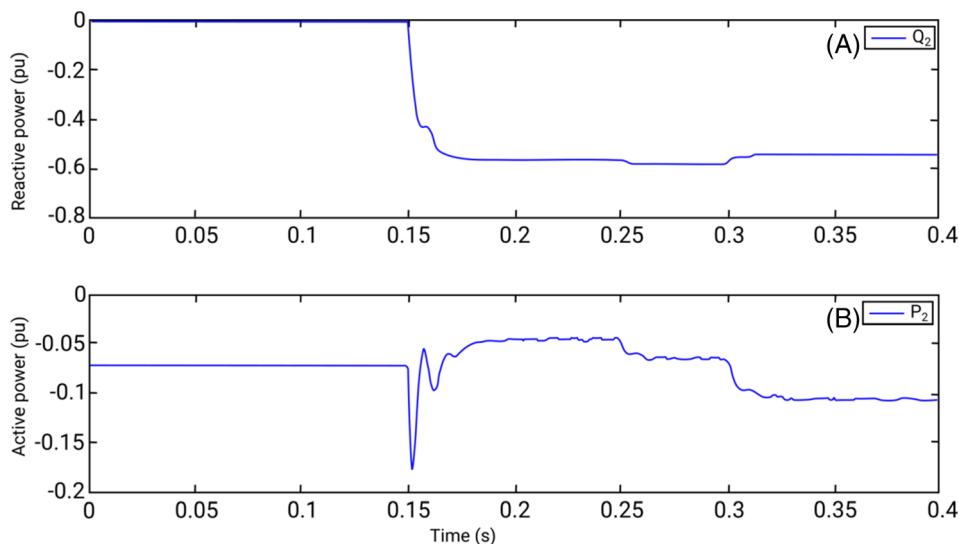


FIGURE 10 Reactive and active powers flowing by AC line 2

### 4.3.2 | Control changing the reference voltages

Given the results obtained by the current control, it is now possible to control the VSC2 through the grid injected series voltage  $v_c$ , acting on  $v_{cd}$  and  $v_{cq}$ . Figure 9 shows how  $v_{cd}$  and  $v_{cq}$  follow the reference voltages  $v_{cd}^*$  and  $v_{cq}^*$  from 0.15 second when the IGBTs are connected. Good tracking of the reference voltages is achieved despite a small coupling between the voltages. Therefore, the voltage control can be used for decreasing or increasing the voltage at the point of connection but does not provide independent control of the active and reactive power flowing to the AC line 2. As shown in Figure 10,  $P_2$  and  $Q_2$  are not decoupled correctly. For this reason, power control is analyzed in the next section.

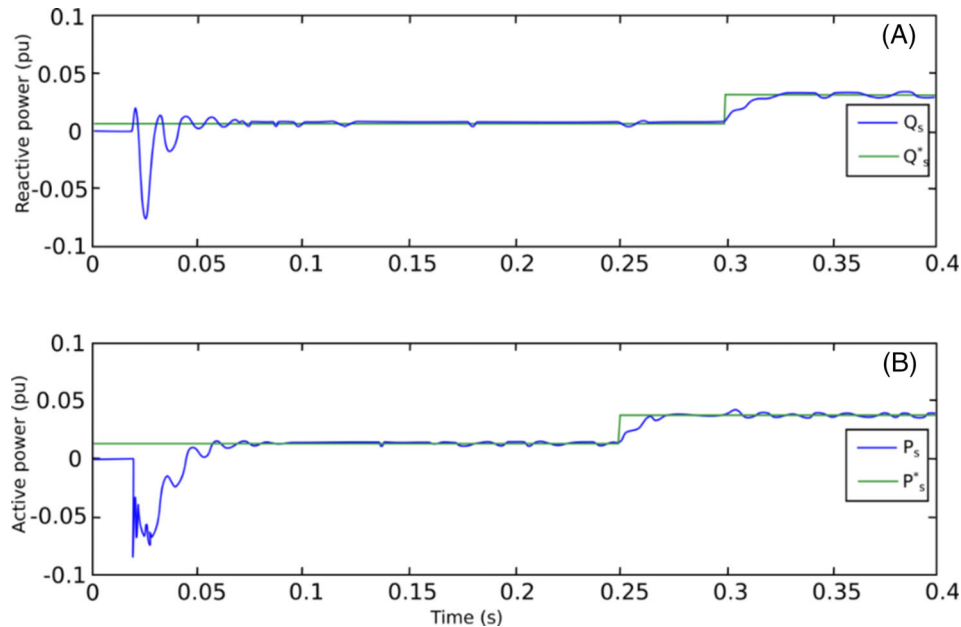


FIGURE 11 Tracking of reference powers  $Q_s^*$  (top) and  $P_s^*$  (bottom)

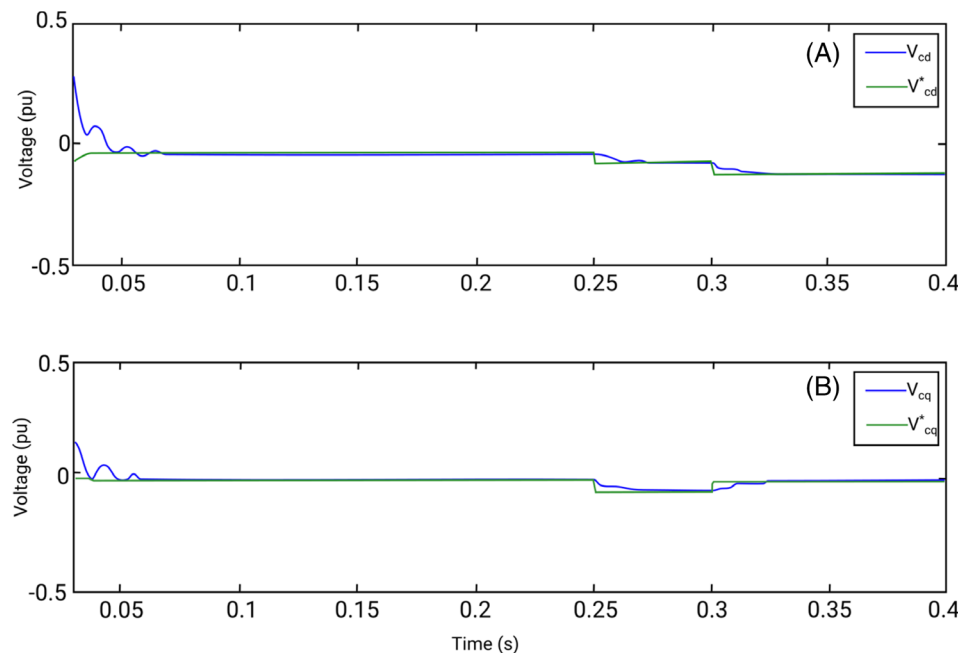


FIGURE 12 Tracking of reference voltage  $v_{cd}^*$  (top) and reference voltage  $v_{cq}^*$  (bottom)

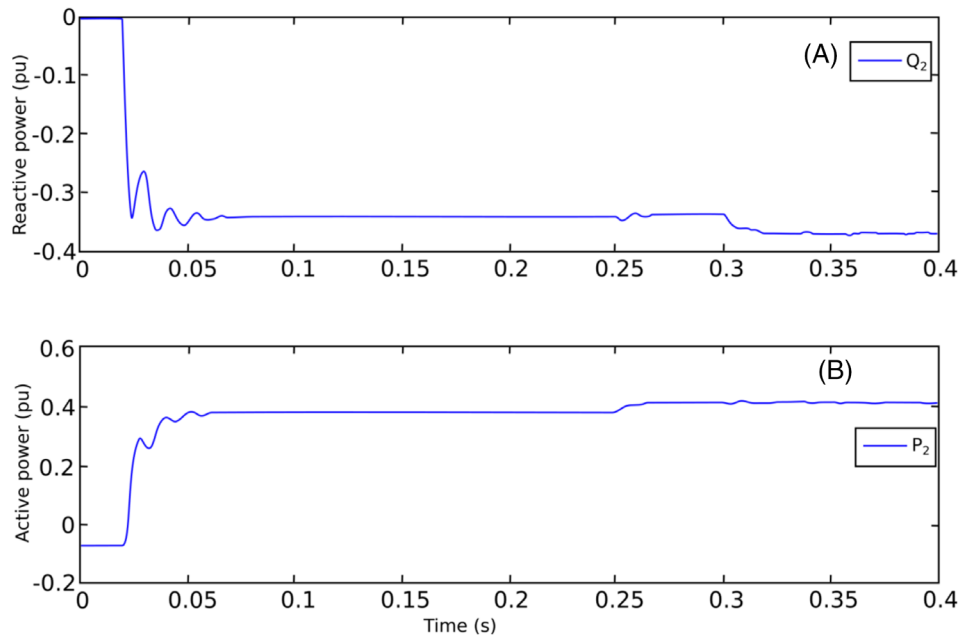


FIGURE 13 Tracking of reactive power  $Q_2$  (top) and active power (bottom)

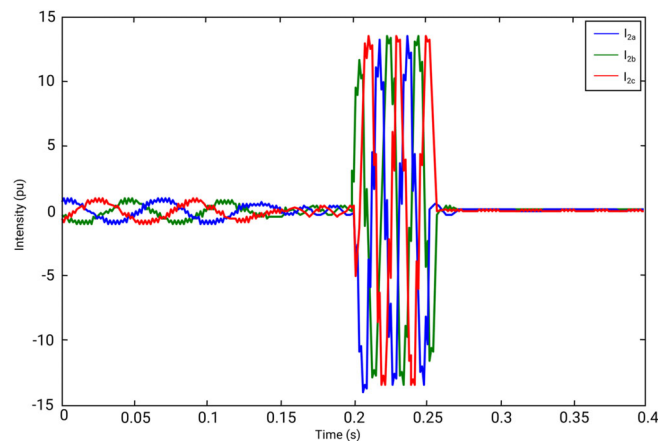


FIGURE 14 Three-phase short-circuit on AC line 2,  $i_2$

### 4.3.3 | Control changing the reference powers

As in the previous section, it is intended to control  $P_2$  and  $Q_2$  via the voltages  $v_{cd}$  and  $v_{cq}$ , but introducing an intermediate step that consists of controlling the powers  $P_s$  and  $Q_s$  with VSC2 (Figure 1) through reference power  $P_s^*$  and  $Q_s^*$ .

Controlling  $P_s$  and  $Q_s$  (Figure 11), the reference voltages  $v_{cd}^*$  and  $v_{cq}^*$  are obtained (Figure 11), and their variations, followed by the voltages  $v_{cd}$  and (Figure 12) will cause  $P_2$  and  $Q_2$  to vary more independently (Figure 13). It can be observed how a variation of  $P_s$  produces a change of  $P_2$  (0.25 second), and a variation of  $Q_s$  modifies  $Q_2$  (0.3 second). A small coupling is maintained between the powers because a change in one of them is reflected in the other. This VSC2 control is more adjusted to make the control of active and reactive powers independent than the controls explained in the previous sections. This does not mean that the above-mentioned strategies could not be valid, because depending on the operational needs, one or the other control strategy could be used.

## 4.4 | Response to a three-phase short-circuit at VSC1

This section studies the behavior of the UPFC topology when a fault occurs at VSC1 terminals. VSC1 is chosen for being the most critical one since it controls the DC link voltage. The short circuit is produced at 0.2 second to ensure a steady-state operation of UPFC before any control strategy is applied, and ends 0.05 second later.

When the fault occurs, the reference voltages  $v_{cd}^*$  and  $v_{cq}^*$  are canceled and the series transformer at VSC2 side is short-circuited. Very high currents are established at 0.2 second due to the short circuit produced at VSC1 terminals, which controls  $v_{dc}$ .  $i_2$  is higher due to the line linking the parallel connection with the UPFC series and for being supplied by a voltage source of 20 kV. This causes the tripping at 0.25 second of the circuit breaker protecting the VSC2 IGBTs, being  $i_2$  null from that moment, since no series voltage is injected into the system (Figure 14). It can also be observed that this configuration cannot act as fault damping since the only possible action to protect the equipment (due to the high value of  $i_2$ ) is to open the switch at the output of the series transformer.

## 5 | MVDC BEHAVIOR ANALYSIS

### 5.1 | MVDC data

In MVDC topology, VSC1 and VSC2 are double connected in parallel (Figure 2). The nominal values that define the converters are shown in Table 2. As in the case of UPFC technology, these data were fixed after consulting with technologists from two companies who were provided with data on the connection point. The following sections show the results obtained for MVDC simulation for both converters and the response to a three-phase short-circuit at VSC1.

### 5.2 | Control changing the reference currents

In this analysis, VSC1 controls  $v_{dc}$  and  $i_{1d}$ , while VSC2 controls  $i_{2d}$  and  $i_{2q}$ . It will be observed how  $P_2$  and  $Q_2$  are controlled independently via  $i_{2q}$  and  $i_{2d}$ , respectively. The change in references for currents and voltages follows the following sequence:

- First, the DC link is preloaded with an uncontrolled rectifier, up to a voltage close to the nominal voltage.
- At 0.3 second, the control over the converters begins. At this point, the IGBTs receive an opening signal. The reference currents are null at the same time as the voltage  $v_{dc}$  is assigned a value higher than that obtained by the uncontrolled rectifier.
- At 0.43 second, a change is applied in the reference current  $i_{1d}^*$ .
- At 1.35 seconds, a change is applied in the reference current  $i_{2d}^*$ .
- At 2.1 seconds, a change is applied in the reference current  $i_{2q}^*$ .

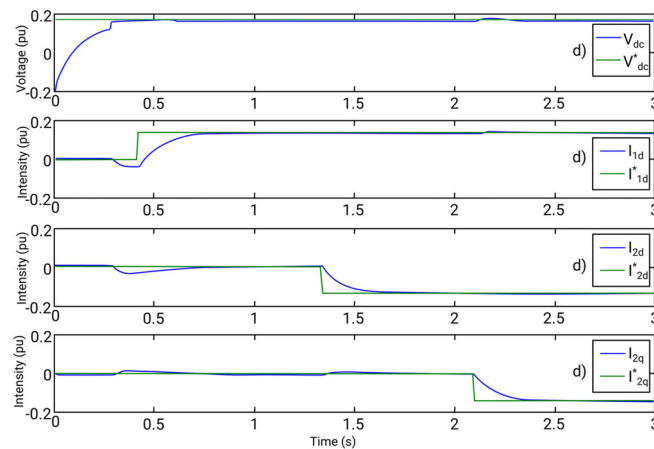


FIGURE 15 Tracking of voltage  $v_{dc}$  and currents  $i_{1d}$ ,  $i_{2d}$ , and  $i_{2q}$

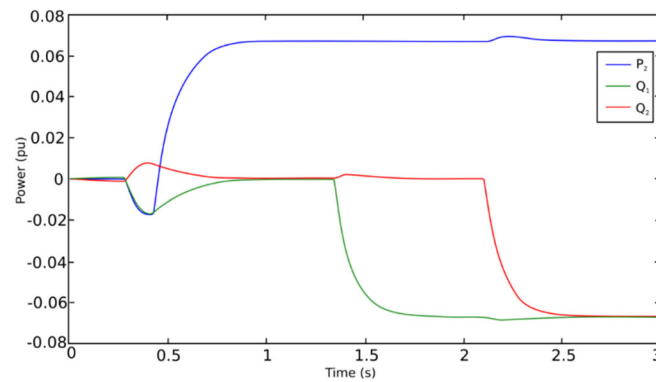


FIGURE 16 Active and reactive power flows

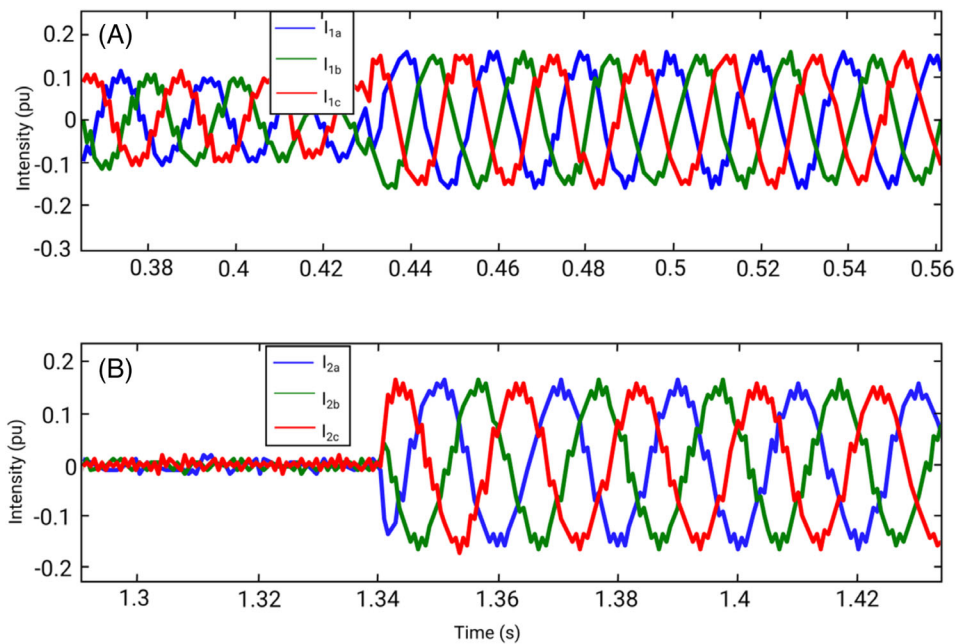


FIGURE 17 Three-phase currents on AC line 1,  $i_1$  (top) and AC line 2,  $i_2$  (bottom)

Before 0.3 second, while the link capacitor is being charged, the reference currents remain null. In Section 4.2, the currents were not blocked until the IGBTs came into operation, and for this reason, the oscillations shown in Figure 5 occurred. Now, in this case, the currents (0.3 second) are blocked, so there is no oscillation (Figure 15). From 0.3 second onwards, the converters start to operate, absorbing VSC1 and VSC2 reactive power since the voltage on AC lines 1 and 2 is higher than on VSC1 and VSC2 terminals, respectively (blue and green lines in Figure 16). Besides, VSC1 absorbs active power, and therefore (neglecting losses), VSC2 supplies active power to the same extent.

At 0.43 second,  $i_{1d}^*$  changes forcing VSC1 to supply reactive power to AC line 1. This means that the voltage on VSC1 terminals becomes higher than the voltage on line 1, so  $v_{dc}$  also increases. This increment of  $v_{dc}$  implies an increase of the voltage at VSC2 terminals until it is equal to the voltage on line 2, not being necessary that VSC2 absorbs reactive power from AC line 2 (green line, Figure 16). In addition, it is no longer necessary that VSC1 absorbs as much active power as before, so VSC2 also needs to supply less active power (red line Figure 16). From 1.35 seconds onwards,  $i_{2d}^*$  changes to a negative value so that reactive power is absorbed by VSC2 from AC line 2 (and VSC1 continues to supply reactive power to the network 1 as no reference has changed), showing the independence of the reactive power control by both converters. Finally, it can be observed that from 2.1 seconds onwards, VSC2 starts to absorb active power because  $i_{2d}^*$  changes to a negative value, and this does not affect the reactive power of VSC2 or VSC1.

With this control strategy, it is clear that, despite the reactive power changes in VSC1 and VSC2 and active power changes in VSC2, the responses are independent of each other, thus demonstrating the independence of active and reactive power control in this type of DC link.

Figure 17 shows the currents  $i_1$  and  $i_2$  in three-phase coordinates for the reference currents changes made previously. Sinusoidal circulating currents with harmonic content are shown again due to the switching of the IGBTs.

### 5.3 | Control changing the reference powers

In this section, the simulations corresponding to the changes produced in the reference powers  $P_2^*$  and  $Q_2^*$  are presented, maintaining the control of  $i_{1d}$  by VSC1 to control the reactive power  $Q_1$ . The process to simulate power control in the converters is as follows:

- It begins by preloading the DC link with an uncontrolled rectifier, up to a voltage close to the nominal voltage.
- At 0.3 second, the control over the converters starts. At this moment, the opening signal is sent to the IGBTs. The reference values for the currents will be null at the same time as the DC link voltage is assigned a value higher than that achieved by the uncontrolled rectifier.
- At 0.75 second, the reference power  $P_2^*$  is changed.
- At 1.5 seconds, the reference power  $Q_2^*$  is changed.
- At 2 seconds, the reference current  $i_{1d}^*$  is changed.

Starting from 0.3 second, when the IGBTs come into operation, the VSC2 supplies active power and absorbs reactive power from AC line 2, as in Section 5.2 since nothing has changed regarding VSC2. For VSC1, it can be observed (Figure 18) that a negative value in the reference current  $i_{1d}^*$  is imposed at 0 s, and the current  $i_{1d}$  is guided toward that reference. This means that it will absorb reactive power (according to the convention adopted for the MVDC) as shown in Figure 19. At 2 seconds, the reference current  $i_{1d}^*$  changes to positive, so VSC2 supplies reactive power, and the values of  $P_2$  and  $Q_2$  are not altered.

In short, as in the previous section, each of the changes in the reference powers is perfectly followed by the converters. Therefore, it is concluded that for MVDC the reference current control and the reference power control allow

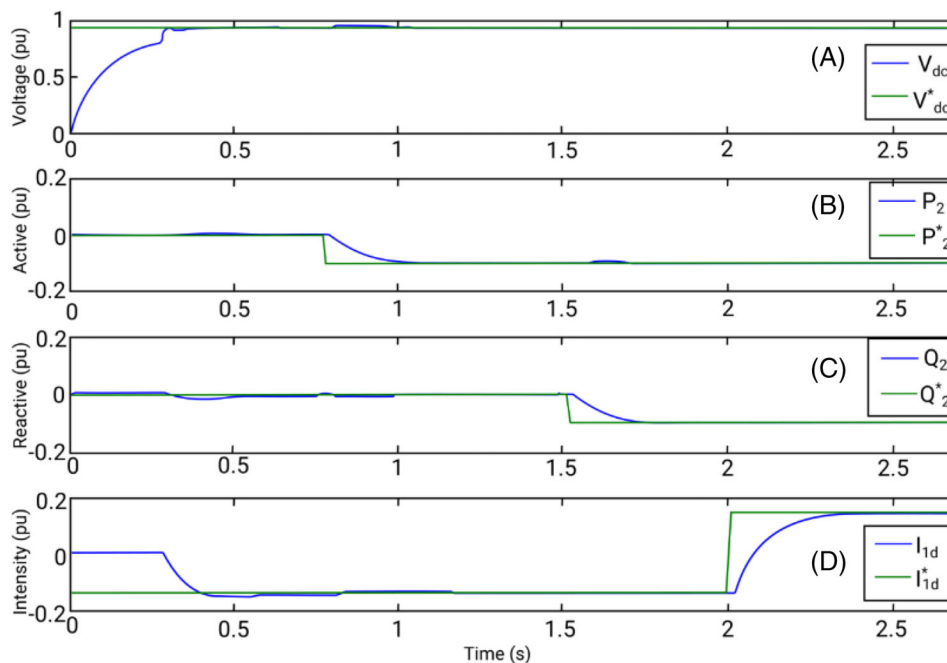


FIGURE 18 Tracking of  $v_{dc}^*$ ,  $P_2^*$ ,  $Q_2^*$  and  $i_{1d}^*$

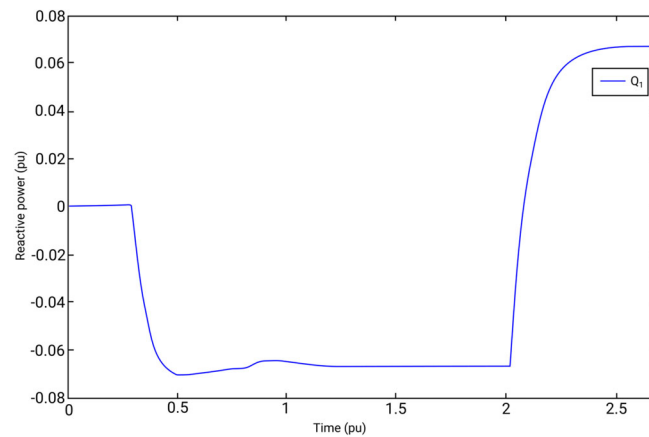


FIGURE 19 Reactive power flow through AC line 1

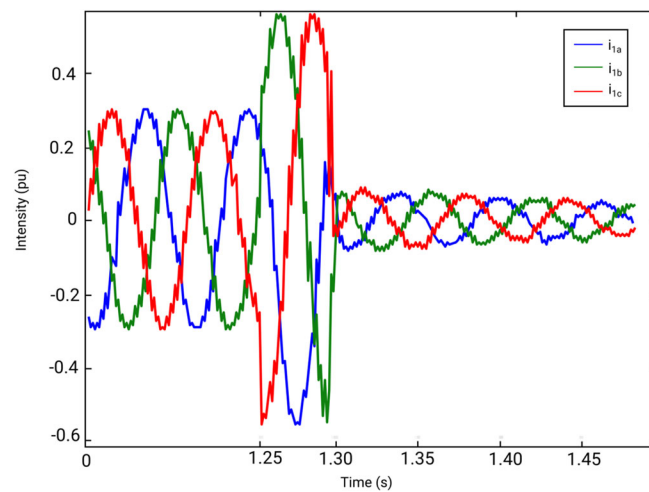


FIGURE 20 Three current in the AC line  $i_1$

independent active and reactive power control, while for UPFC this is only achieved with the control changing the reference powers, and not entirely due to the small coupling between them.

#### 5.4 | Response to a three-phase short-circuit at VSC1

In this section, the performance of MVDC is studied when a fault occurs at VSC1 terminals since this is the most critical converter due to its control of  $v_{dc}$ . The conditions of the simulated short-circuit are the same as for UPFC in Section 4.4.

When the fault occurs, VSC1, which was controlling  $v_{dc}$ , is not able to maintain that voltage, being now  $v_{dc}$  controlled by VSC2. With that purpose, VSC2 absorbs reactive power to increase the voltage at its terminals as well as  $v_{dc}$ . At 1.30 seconds, and since  $v_{dc}$  was stabilized, it is no longer necessary to pursue the strategy described above for dynamic operation, so it switches to strategy in a stationary mode where VSC1 monitors  $v_{dc}$  again. From 1.30 seconds, the voltage at VSC1 terminals increases too, in the same ratio in which  $v_{dc}$  did, thanks to being controlled by VSC2 (just before 1.30 seconds, the voltage at VSC1 terminals was null due to the fault). As a result, the VSC1 input short-circuit current is dampened (Figure 20) while continuing to supply VSC2 terminals, since there was not necessary to clear it through the line protections that act on the main circuit breakers of the continuous link, as was the case in Section 4.4 when UPFC was used.

It can be observed in Figure 20 how  $i_1$  increases at 1.25 seconds due to the fault and the fast operation of the controllers, keeping the currents low in order not to supply the short-circuit current, as opposed to Section 4.4 for UPFC, which simply cuts off supply to clear the fault.



## 6 | CONCLUSION

The increase in electrical demand and the incorporation of distributed energy resources into the distribution grids is causing power systems to start working close to their technical limits. In this global context, it is necessary to propose solutions that involve a change in the way electrical grids are planned and operated. The incorporation of MVDC devices in MV grids can be an optimal solution to this problem. MVDC brings numerous benefits, allowing power flows to be dynamically forced and to make better use of existing grid capacity.

To show the benefits of this technology, an MVDC device has been analyzed simulating a real situation in a congested distribution grid, comparing it with a UPFC device, both based on the use of VSC converters.

First, a dynamic simulation of both topologies has been carried out, studying separately the control of each one of them with different variations of their parameters. The drawn conclusions are:

- It has been shown that the tracking of the reference signals of the parameters in both devices is good. However, the objective of decoupling active and reactive power control by variation of the control parameters is perfectly satisfied by the MVDC topology, whereas the UPFC only achieves it in the case of power parameter variation
- Subsequently, the behavior of MVDC and UPFC has been analyzed in the case of a three-phase short circuit in terminals of the VSC1, which controls the DC link voltage, as this is the most severe fault. It has been shown that UPFC is not capable of dampening the fault, being the only action possible to remove it from service, while MVDC allows acting on the currents circulating through the electrical line mitigating the effect caused by the fault.

Therefore, it has been shown that the implementation of MVDC in distribution networks can help, better than other options, solve some of the problems that these networks are currently experiencing.

In a future work, this research aims to further study the selection of the most appropriate nodes for the location of the links, including economic aspects in the optimization criteria, and to continue analyzing real situations in which this technology can be applied.

### PEER REVIEW

The peer review history for this article is available at <https://publons.com/publon/10.1002/2050-7038.13038>.

### DATA AVAILABILITY STATEMENT

The dataset generated during the study is not available due to the internal policy of the distributor company. Data has only been provided for the performance of this study and subsequent work that is intended to be done.

### ORCID

Oscar Duque-Perez  <https://orcid.org/0000-0003-2994-2520>

### REFERENCES

1. Eltigani D, Masri S. Challenges of integrating renewable energy sources to smart grids: a review. *Renew Sustain Energy Rev.* 2015;52:770-780. <https://doi.org/10.1016/j.rser.2015.07.140>
2. Li Y, Tian X, Liu C, et al. Study on voltage control in distribution network with renewable energy integration. Paper presented at: IEEE Conference on Energy Internet and Energy Systems Integration (EI2); November 2017; Beijing, China. <https://doi.org/10.1109/EI2.2017.8245755>.
3. Zhang X, Lu C, Liu S, et al. A review on wide-area damping control to restrain inter-area low frequency oscillation for large-scale power systems with increasing renewable generation. *Renew Sustain Energy Rev.* 2016;57:45-58. <https://doi.org/10.1016/j.rser.2015.12.167>
4. Gyugyi L, Rietman R, Edris A, et al. The unified power flow controller: a new approach to power transmission control. *IEEE Trans Power Deliv.* 1995;10:1085-1097. <https://doi.org/10.1109/61.400878>
5. Maza-Ortega JM, Acha A, García S, et al. Overview of power electronics technology and applications in power generation transmission and distribution. *J Modern Power Syst Clean Energy.* 2017;5(4):499-514. <https://doi.org/10.1007/s40565-017-0308-x>
6. Jin Z, Sulligoi G, Cuzner R, et al. Next-generation shipboard DC power system. *IEEE Electrif Magazine* 2016. Vol 4. 2. p. 45-57. DOI: <https://doi.org/10.1109/MELE.2016.2544203>
7. Pinto RT, Bauer P, Rodrigues SF, et al. A novel distributed direct-voltage control strategy for grid integration of offshore wind energy systems through MTDC network. *IEEE Trans Indus Electron Junio* 2013. Vol 60. 6. p. 2429-2441. DOI: <https://doi.org/10.1109/TIE.2012.2216239>
8. Gómez-Expósito A, Mauricio JM, Maza-Ortega, JM. VSC-based MVDC railway electrification system. *IEEE Trans Power Deliv* 2014. Vol. 29, 1. p. 422-431. DOI: <https://doi.org/10.1109/TPWRD.2013.2268692>

9. Verdicchio A, Ladoux P, Caron H, et al. New medium-voltage DC railway electrification system. *IEEE Trans Transport Electrification*, Vol. 4, N° 2, pp. 591–604. 2018. DOI: <https://doi.org/10.1109/TTE.2018.2826780>
10. Bathurst G, Hwang G, Tejwani L. MVDC – the new technology for distribution networks. Paper presented at: 11th IET International Conference on Power Transmission AC and DC. February 2015; Birmingham, UK. <https://doi.org/10.1049/cp.2015.0037>.
11. Mesas JJ, Monjo LI, Sainz L, et al. Study of MVDC system benchmark networks. Paper presented at: *International Symposium on Smart Electric Distribution System and Technologies (EDST)*. Vienna, Austria; 2015. <https://doi.org/10.1109/SEDST.2015.7315213>
12. Larruskain DM, Zamora I, Abarrategui O, et al. VSC-HVDC configurations for converting AC distribution lines into DC lines. *Int J Electr Power Energy Syst*. 2014;54:589–597. <https://doi.org/10.1016/j.ijepes.2013.08.005>
13. Zhang L, Liang J, Tang W, et al. Converting AC distribution lines to DC to increase transfer capacities and DG penetration. *IEEE Trans Smart Grid*. 2019;10(2):1477–1487. <https://doi.org/10.1109/TSG.2017.2768392>
14. Qi Q, Long C, Wu J, et al. Using an MVDC link to increase DG hosting capacity of a distribution network. *Energy Procedia*. 2017;142: 2224–2229. <https://doi.org/10.1016/j.egypro.2017.12.622>
15. Bryans R, Bebbington M, JYu J, et al. Real time control of a distribution connected MVDC link (ANGLE-DC). Paper presented at: 13th IET International Conference on AC and DC Power Transmission (ACDC); May 2017; Manchester, UK. <https://doi.org/10.1049/cp.2017.0003>.
16. Hunter L, Booth C, Finney S, et al. MVDC network balancing for increased penetration of low carbon technologies. Paper presented at: 8th IEEE PES Innovative Smart Grid Technologies Conference Europe (ISGT-Europe); October 2018; Sarajevo, Bosnia-Herzegovina. <https://doi.org/10.1109/ISGTEurope.2018.8571838>.
17. Han C, Song S, Kim J, et al. Enhancing line capacity utilization in power transmission system using active MVDC link. *Energies*. 2019;12(9):1–23. <https://doi.org/10.3390/en12091589>
18. Ji Y, Yuan Z, Zhao J, et al. Overall control scheme for VSC-based medium-voltage DC power distribution networks. *IET Gener Transm Distrib*, vol 12, 6, pp. 1438–1445. 2018. DOI: <https://doi.org/10.1049/iet-gtd.2017.0912>
19. Stieneker M, De Doncker RW. Medium-voltage DC distribution grids in urban areas. Paper presented at: IEEE 7th International Symposium on Power Electronics for Distributed Generation Systems (PEDG); June 2016; Vancouver, Canada. <https://doi.org/10.1109/PEDG.2016.7527045>.
20. Chiandone M, Sulligoi G, Milano F, et al. Back-to-Back MVDC link for distribution system active connection. A network study. Paper presented at: 3rd International Conference on Renewable Energy Research and Applications (ICRERA); January 2015; Milwaukee, WI. <https://doi.org/10.1109/ICRERA.2014.7016536>.
21. Reddy AK, Singh SP. Congestion mitigation using UPFC. *IET Gener Transm Distrib*, vol 10, 10, pp. 2433–2442. 2016. DOI: <https://doi.org/10.1049/iet-gtd.2015.1199>
22. Boyra M, Thomas J-L. Size comparison of MVDC and D-UPFC for MV distribution network interconnection. Paper presented at: SPEEDAM 2010; 2010; Pisa, Italia:245–250. <https://doi.org/10.1109/SPEEDAM.2010.5545064>.
23. Ken AJF, Mehraban AS, Lombard X, et al. Unified power flow controller (UPFC) modeling and analysis. *IEEE Trans Power Deliv*, vol 14, 2, pp. 648–654. 1999. DOI: <https://doi.org/10.1109/61.754113>
24. Shahgholian G, Mahdavian M, Janghorbani M, et al. Analysis and simulation of UPFC in electrical power system for power flow control. Paper presented at: 14th International Conference on Electrical Engineering/Electronics, Computer, Telecommunications and Information Technology (ECTI-CON); June 2017; Phuket, Thailand. <https://doi.org/10.1109/ECTICon.2017.8096173>.
25. Waghade SN, Gowder C. Enhancement of power flow capability in power system using UPFC- a review. *Int Res J Eng Technol*. 2019;6: 1146–1150. <https://doi.org/10.18178/ijeee.4.3.199-202>
26. Yang J, Xu Z. Power flow calculation methods for power systems with novel structure UPFC. *Appl Sci*. 2020;10(15):5121. <https://doi.org/10.3390/app10155121>
27. Shen X, Luo H, Gao W, et al. Evaluation of optimal UPFC allocation for improving transmission capacity. *Global Energy Interconnection*. Volume 3 3, pp. 217–226. 2020. DOI: <https://doi.org/10.1016/j.gloi.2020.07.003>
28. Song P, Xu Z, Dong H, et al. Security-constrained line loss minimization in distribution systems with high penetration of renewable energy using UPFC. *J Modern Power Syst Clean Energy*, vol 5, 6, pp. 876–886. 2017. DOI: <https://doi.org/10.1007/s40565-017-0334-8>
29. Cai H, Yang L, Wang H, et al. Application of unified power flow controller (UPFC) in Jiangsu power system. Paper presented at: Proceedings of the 2017 IEEE Power & Energy Society General Meeting; July 2017; Chicago, USA:1–5. <https://doi.org/10.1109/PESGM.2017.8274211>.
30. L Pi, Wang PY, Feng C, et al. Application of MMC-UPFC in the 500 kV power grid of Suzhou. *J Eng* Vol 2017, 13, pp. 2514–2518. 2017. doi: <https://doi.org/10.1049/joe.2017.0780>
31. Cui Y, Yu Y, et al. Analysis of application effect of 220 kV UPFC demonstration project in Shanghai grid. *J Eng* Vol 2019, 16, pp. 136–142. 2018. DOI: <https://doi.org/10.7667/PSPC170565>
32. Giannakis A, Peftitsi D. MVDC distribution grids and potential applications: future trends and protection challenges. Paper presented at: 20th European Conference on Power Electronics and Applications (EPE'18 ECCE Europe); September 2018; Riga, Latvia.
33. Zorita-Lamadrid AL, De La Rubia-Herrera A, Duque-Perez O, et al. Medium voltage direct current (MVDC), a new system for the management and operability of electricity distribution grids. *DYNA* Vol 95, 6, pp. 579–582. 2020. DOI: <https://doi.org/10.6036/9493>
34. Zuelli R, Chiumeo RGM, Gandolfi C, et al. The impact of MVDC links on distribution networks. Paper presented at: AEIT International Annual Conference; October 2018; Bari, Italy. <https://doi.org/10.23919/AEIT.2018.8577442>.
35. Alcalá J, Charre S, Durán M, et al. Analysis of the Back to Back converter for power flow management. *Inf Tecnol*, vol 25, n°6, pp. 109–116. 2014 DOI: <https://doi.org/10.4067/S0718-07642014000600014>

36. Fu Y, Yeleti S, Abdelwahed S, et al. Optimal operation of multi-terminal VSC based MVDC power distribution systems. Paper presented at: International Conference on High Voltage Engineering and Application; September 2012; Shanghai, China. <https://doi.org/10.1109/ICHVE.2012.6357054>.
37. Simiyu P, Xin A, Bitew GT, et al. Review of the DC voltage coordinated control strategies for multi-terminal VSC-MVDC distribution network. *J Eng*, vol. 2019, 16, pp. 1462–1468. 2019. DOI: <https://doi.org/10.1049/joe.2018.8841>
38. Qu L, Yu Z, Song Q, et al. Planning and analysis of the demonstration project of the MVDC distribution network in Zhuhai. *Energy* 2019, Vol. 13, n°1, pp. 120–130. DOI:<https://doi.org/10.1007/s11708-018-0599-2>
39. Alcalá J, Cárdenas V, Espinoza J, et al. Investigation on the limitation of the BTB-VSC converter to control the active and reactive power flow. *Electr Pow Syst Res*. 2017;143:149-162. <https://doi.org/10.1016/j.epsr.2016.09.012>
40. Salman GA, Ali MH, Abdullah AN. Implementation optimal location and sizing of UPFC on Iraqi power system grid (132 kV) using genetic algorithm. *Int J Power Electron Drive Syst*. 2018;9(4):1607-1615. <https://doi.org/10.11591/ijpeds.v9.i4.pp1607-1615>
41. Radu D, Besanger Y. A multi-objective genetic algorithm approach to optimal allocation of multi-type FACTS devices for power systems security. Paper presented at: 2006 IEEE Power Engineering Society General Meeting; June 2006. <https://doi.org/10.1109/PES.2006.1709202>.

**How to cite this article:** de la Rubia Herrera A, Zorita-Lamadrid AL, Duque-Perez O, Morinigo-Sotelo D. Analysis of the behavior of MVDC system in a distribution grid compared to a UPFC system. *Int Trans Electr Energ Syst*. 2021;e13038. <https://doi.org/10.1002/2050-7038.13038>